AADE-07-NTCE-35

Bit Hydraulics Optimization with Variable Rheological Properties

Mario Zamora and Sanjit Roy, M-I SWACO

Abstract

The bit hydraulics optimization process is improved when drilling fluid rheological properties, historically considered input variables, instead become key goals of the optimization effort. This serves to decouple constraints that previously could unwittingly skew the results. Described in this paper are the benefits, requirements, and difficulties of determining the best Herschel-Bulkley parameters while simultaneously satisfying pre-defined optimization criteria and boundary conditions. Hydraulic window concepts are used to illustrate the overall process and companion software. Case histories are included that demonstrate improvements in hydraulic efficiency by optimizing fluid rheological properties.

On a practical level, bit hydraulics optimization seeks to find a flow rate that maximizes a selected fluid-power criterion while considering a host of real or given physical limits and constraints. Jet-bit nozzles (or total flow area) are then sized to match a desired pump pressure. Common constraints including drilling margin, hole cleaning, and barite-sag requirements, pump horsepower, and others create two well-known, distinctive hydraulic windows bounded by flow rates and pressure limitations. Trial-and-error and special software convergence techniques are required to determine optimum rheological properties because of the combined effects of temperature and pressure profiles and other complex downhole conditions.

Introduction

The underlying objective of bit hydraulics optimization is to promote high drilling rates by delivering the necessary hydraulic energy beneath the bit to clean the mud-rock interface, rapidly remove cuttings around the bit face, and create crossflow to minimize cuttings regrinding.[1] Powerful mud pumps, quality bit designs, and fit-for-purpose jet-nozzle configurations contribute significantly in this regard.[2,3,4]

Optimization occurs when the total available system energy is proportioned to maximize available hydraulic energy at the bit. Theoretical relationships that maximize bit hydraulic horsepower, impact force, and jet velocity were first published by Kendall and Goins.[5] They stressed the need to consider "all necessary restrictions on operating conditions", provided procedures for maximizing the different criteria, and presented a graphical method for determining flow rates and sizing nozzles. Subsequent publications[6,7,8,9] on this subject have presented worthy variations on the original theme.

Other publications are notable because of their emphasis on field implementation. For example, the innovative optimization approach published by Scott[10] takes advantage of field measurements, a technique later popularized by a handy optimization slide rule.[11] Also, practical guidelines such as those from Randall[12] have proven particularly valuable for placing key issues and parameters in proper perspective.

Critical characteristics of many of today's wells, on the other hand, have made it advantageous and even necessary to rely on computer technology to execute the bit hydraulics optimization process. Swanson, *et al.*[13] are among those that have advocated this approach, especially when considering a large number of parameters. Reduction in the number of parameters can simplify computer algorithms and increase chances of converging on a solution, particularly when multiple, narrow boundary conditions are involved. However, unnecessary predefinition of key independent variables can lead to less-than-optimal results.

Drilling fluid rheological properties are among the important parameters that invariably are fixed input values. These properties, however, affect so many aspects of the hydraulics system that there can be great value in making them a more active part of the hydraulics planning process. Flexibility clearly is limited during drilling, but this does not diminish the impact of rheological properties on overall goals.

This paper presents the application of a hydraulics program where optimization goals include Herschel-Bulkley rheological parameters as would be measured at the surface with a standard field viscometer. The overall process, illustrated using familiar hydraulic windows concepts, involves complex relationships for variable downhole properties and conditions along the lines of those provided by the modernized version of *API RP-13D*.[9] Case studies based on field applications are included to demonstrate improvement opportunities and sensitivity to various conditions and parameters.

Optimization Mechanics

Practically speaking, the bit hydraulics optimization process for most drilling engineers has been distilled to finding the best combination of flow rate and jet-nozzle sizes (or total flow area) that achieve drilling goals while satisfying actual or assumed boundary conditions. More options clearly are available during planning stages, but fewer uncertainties exist while drilling is in progress. In either case, the

optimization process suffers when boundary conditions are too restrictive, sometimes resulting in compromises on many of today's most critical wells.

Graphic "windows" have long been effective as tools to visualize, analyze, and optimize the process. Two well-known hydraulics windows are used in this paper to visually demonstrate relationships among various parameters and boundary conditions. They also revisit basic concepts to help counteract an apparent loss of understanding and appreciation of bit hydraulics optimization in recent years.

The first window illustrates relationships among annular pressure losses, drilling margin, and critical flow-rate limitations based on well conditions and pump capabilities. The second is the classic graphic used primarily to determine the flow requirements to maximize a selected optimization criterion at the bit. The two windows are inescapably linked by the flow-rate range, which depends on mud rheology.

Annular Hydraulics Window. The Annular Hydraulics Window shown in Fig. 1a is a useful tool to help define and illustrate requirements for maintaining a non-obstructed, gauge, quality wellbore without mud losses or other stability issues. Within the context of this paper, its primary goal is to establish the flow-rate range based on different rheological properties that can be shared with the Bit Hydraulics Optimization Window (Fig. 1b) discussed in the next section.

The Annular Hydraulics Window is a plot of equivalent circulating density at the casing shoe *ECD* versus flow rate *Q*). For some, it is convenient to use ΔECD as the dependent variable, but this is a matter of choice. Pressure and flow-rate limits which form the perimeter of the centerpiece rectangular "window" are surprisingly interrelated by way of the drilling fluid rheology.

Drilling margin is represented by upper and lower limits defined by the fracture gradient at the casing shoe *FG* and the equivalent static density *ESD*. *ESD*, the static downhole mud weight adjusted for temperature and pressure, incorporates pore pressure and wellbore stability issues.[14]

The left and right window borders define the available flow rate range. The left edge is the minimum flow rate *Qmin* which depends primarily on rig pump limits and hole-cleaning/barite-sag requirements.[9] The right boundary is the maximum flow rate *Qmax* defined by the lowest value determined from the onset of turbulence, maximum pump output, consumption of pump pressure as parasitic losses, and the intersection of the ECD-with-cuttings curve with the *FG* boundary. The latter is the case for the example illustrated in Fig. 1a. For very narrow drilling margins, like those encountered in many deepwater and HTHP wells, the flow-rate range is squeezed such that the wells cannot be safely drilled without modifying mud properties or controlled drilling as a last resort.

The notable dependency of this window on rheology provides the opportunity for finding the best properties to satisfy the multitude of boundary conditions. Pre-defining mud rheological parameters as input values (by plan or by ignoring the possibility of field adjustments) could unnecessarily restrict the optimization process.

Bit Hydraulics Optimization Window. The Bit Hydraulics Optimization graph in Fig. 1b also is constructed around a rectangular "window" defined by pressure and flow-rate limits. In this case, system pressures *P* is the dependent variable and the data are plotted on log-log coordinates. Detailed descriptions and use of this window are available elsewhere.[6,8,9,10,11] The brief discussion provided here highlights the impact of mud rheology on the overall optimization process.

Pump pressure *Pp* so indicated as the upper boundary of the window is a critical element of the optimization process. Relationships presented below require that *Pp* be constant, independent of flow rate. Minimum and maximum flow rates carried over from the Annular Hydraulics Window are shown as left and right vertical edges of the rectangle.

Log coordinates are used so that two key power curves can be constructed as straight lines. The first is the available pump hydraulic horsepower *HHPp* defined by

$$Pp = 1714(HHPp)Q^{-1} \quad \text{... (1)}$$

If the *HHPp* line cuts across the window (usually near the upper, right-hand corner), Eq. 1 must be checked so that the combination of *Pp* and *Q* does not exceed the maximum hydraulic horsepower of the pump.

The second power curve represents system pressure losses excluding the bit. It is generally accepted that the so-called parasitic pressure loss *Px* is proportional to Q^s, where the exponent *s* varies from about 1.3 to 1.9 depending on the turbulent flow characteristics of the drilling fluid and drill string geometry. The exponent *s* can be determined empirically from measured field data,[10] modeled,[9] or a default value.

The most commonly used default values for the turbulent flow behavior index *s* are 1.86 and 1.75, derived from two different Blausius-style, friction-factor relationships that appear throughout the literature. Kendall and Goins[5] used *s* = 1.9 to develop their well-known conditions for maximizing bit hydraulics for three different criteria, under conditions of a constant pump pressure:

- Maximum Bit Hydraulic Horsepower (*HHPb*)

$$Pb = \left(\frac{s}{s+1}\right)Pp = 0.655\,Pp \approx \frac{2}{3}Pp \quad \text{... (2)}$$

$$Px = \left(\frac{1}{s+1}\right)Pp = 0.345Pp \approx \frac{1}{3}Pp \quad \text{... (3)}$$

- Maximum Bit Impact Force (*IFb*)

$$Pb = \left(\frac{s}{s+2}\right)Pp = 0.487Pp \approx \frac{1}{2}Pp \quad \text{... (4)}$$

$$Px = \left(\frac{2}{s+2}\right)Pp = 0.513Pp \approx \frac{1}{2}Pp \quad \text{... (5)}$$

- Maximum Jet Velocity (*Vj*)

$$Pb = Pp - Px \,@\, Q_{\min} \quad \text{... (6)}$$

Despite the general acceptance ⅔*Pp* and ½*Pp* for maximum *HHPb* and *IFb*, respectively, Table 1 demonstrates that the turbulent flow behavior index *s* can theoretically lower by as much as 10% the bit pressure loss required for optimization. Unfortunately, the range for *s* can be difficult to pin-point because of the effects of mud composition, drag reduction (in turbulent flow), and combined laminar-turbulent losses at lower flow rates. Definitive data on this issue have yet to be published.

Basically speaking, optimization based on *HHPb* and *IFb* first determines the flow rate *Qopt* for which *Px* matches the criterion in Eq. 3 or Eq. 5. This can be done graphically as demonstrated in Fig. 1b or using analytical methods.[9]

The optimum flow rate *Qopt* would have to exist within *Qmin* and *Qmax* for an optimum or maximum solution. For this case, the recommended flow rate *Qrec* = *Qopt*. Otherwise, for *Qopt* ≤ *Qmin*, then *Qrec* = *Qmin*; for *Qopt* ≥ *Qmax*, then *Qrec* = *Qmax*. In these latter cases, *HHPb* or *IFb* would be maximized, but not theoretically optimized. As indicated by Eq. 6, maximum jet velocity *Vj* results when *Qrec* = *Qmin*.[5]

As illustrated in Fig. 1b, *Qopt* for *IFb* exceeds *Qmax*, meaning that *Qrec* = *Qmax* for this criterion. Fig. 2 is another way of showing this. The decreasing horsepower and impact-force values after their respective peaks demonstrate the rapid increase in parasitic losses at high flow rates under a constant pump pressure. For this example, the pump pressure is entirely lost to parasitic pressures as the flow rate approaches 650 gal/min. This represents the absolute maximum flow rate.

The next step determines the available bit pressure loss *Pb* by subtracting *Px@Qrec* from the pump pressure *Pp*. Nozzles (or total flow area) can then be calculated directly from *Qrec* and *Pb* values.[9] Table 1 summarizes key fluid and optimization parameters for achieving maximum *HHPb*.

Final steps involve comparing results to other boundary conditions and guidelines. For example, guidelines exist for minimum values of HSI (HHPb/in.^{2}) and jet velocity of 4-10 hp/in.^{2} and 300-450 ft/s for water-based muds and 3-6 hp/in.^{2} and 200-350 ft/s for non-aqueous fluids. Clearly, iterative procedures, parameter modifications, and/or compromises could be in order.

Optimization Relationships. Fig. 2 is another way to view relationships among the various optimization criteria and flow rate. The equations for *HHPb*, *IFb*, and *Vj* are monotonic, unbounded functions of Q^3, Q^2, and Q, respectively.[5] However, because parasitic losses increase with flow rate by Q^s, high flow rates mean less available pressure for the bit nozzles at a constant pump pressure. As mentioned earlier and shown in Fig. 2, the 3,500 psi available pump pressure is completely used up at just over 650 gal/min. This is precisely why *HHPb* and *IFb* each pass through a maximum value and maximum *Vj* occurs at the lowest possible flow rate (*Qmin*).

Maximum conditions for each criterion are indicated on Fig. 2. It is notable that the optimum flow rate for maximum jet velocity categorically occurs at the lowest flow rate (240 gal/min for this example), at the middle flow rate for maximum bit hydraulic horsepower, and at the highest flow rate for impact force (460 gal/min). In this case, the flow rate for impact force exceeds the maximum allowable.

Despite concerted efforts, it has not been possible to determine which of the optimization criteria is "best". Because of typical field constraints, however, optimization based on impact force is used more often in large holes at shallow depths where high flow rates are important, bit hydraulic horsepower at depth where parasitic losses are proportionally higher, and jet velocity when narrow drilling margins force low flow rates to minimize annular pressure losses and mitigate lost returns.

Optimization with Variable Rheology

Most available hydraulics optimization procedures use assumed or given mud rheological properties. The significance of presenting the window concepts in the previous section is to illustrate the impact of predefining these rheological properties. *Qmin*, *Qmax*, *ECD*, parasitic losses, and the conditions for theoretical optimization are the parameters most affected.

Using *Qmin* as an example, it helps to imagine a family of complex curves superimposed on Fig. 1 that are independent of rheology. For example, one such family could be a series of hole-cleaning curves based on constant rates of penetration (ROP). The intersection of the ECD-plus-cuttings curve with the actual or planned ROP would establish *Qmin*. Lowering the ECD curve (by decreasing rheology, for example) would increase *Qmin* for the same ROP. However, elevating the ECD curve (by increasing rheology) to reduce *Qmin* could restrict the flow rate in narrow drilling margin operations.

Temperature and pressure effects on downhole density and rheology can further cloud the optimization process. In deepwater applications, for example, the ECD curves could shift upwards due to higher densities in colder temperatures and increased frictional pressure losses. This could create operational difficulties when coupled with the expected narrow drilling margin.

Software Description

The optimization process with variable rheology is considerably more involved and lends itself to computer solution. Primary targets are the Herschel-Bulkley parameters n, k, and τ_y, recommended flow rate *Qrec*, and bit total flow area (TFA) that simultaneously satisfy specified well parameters and optimization criteria. The rheological parameters represent those measured at the surface with conventional viscometers; however, the solution is based on variable downhole properties and conditions.

Explicit solutions are not possible because of the various complexities. Instead, the program systematically and iteratively inspects a wide range of surface-representative rheological properties, concurrently adjusting densities and rheological properties for downhole conditions. A matrix of valid solutions for *Qopt* is created based on the Hydraulic Windows and using a numerical process similar to the graphical process described previously in this paper.

For any given set of simulated Herschel-Bulkley

parameters under surface conditions, the software determines downhole rheology and density profiles using a finite difference scheme. ECD profiles, *Qmin*, and *Qmax* are then generated for each set and used as optimization input. The usually large matrix of possible solutions is then evaluated using convergence techniques to find the most appropriate set for the selected optimization criterion (bit hydraulic power, jet impact force, or jet velocity). Bit nozzles TFA are then sized accordingly to match desired pump pressure.

This approach ensures that all conditions and specifications are considered in the optimization process. There are instances, of course, where an optimal solution is not possible. The most common occurs when the optimum flow rate is insufficient to clean the hole or mitigate barite sag. For these cases, *Qrec* is set to *Qmin*, which still maximizes jet velocity. Cases where adequate hole cleaning cannot be achieved without fracturing the formation are addressed by controlling penetration rates. Insufficient *HSI* values can be corrected by increasing pump pressure.

As a practical matter, the program is designed to iterate over values of plastic viscosity *PV* and yield point *YP* instead of the Herschel-Bulkley parameters. The two sets of values are related by the following:

$$n = 3.32 \log_{10}\left(\frac{2PV + YP - \tau_y}{PV + YP - \tau_y}\right) \quad \ldots(7)$$

$$k = \frac{PV + YP - \tau_y}{511^n} \quad \ldots(8)$$

$$R = \frac{\tau_y}{YP} \quad \ldots(9)$$

Fig. 3 is a partial screen capture that graphically shows results from the iterative process used to evaluate *PV* and *YP* combinations on optimization. The upper set of data failed the criteria during this particular step in the iteration. The lower enclosed data set that passed is used to construct the boundaries for the next iteration. This basic convergence technique continues until all conditions are satisfied, or it is clear that an "optimum" solution cannot be found. A separate process is then initiated to find the best compromise.

The ratio of yield stress to yield point *R* is a useful parameter for indicating general rheological behavior and for achieving convergence. Attempts to vary *PV*, *YP* and τ_y clearly would be daunting. $R = 0$ for power law fluids, $R = 1$ for Bingham plastic fluids, and $0 < R < 1$ for Herschel-Bulkley fluids. In the computer program, *R* is used to suggest values for τ_y used during the iteration procedure.

In an evaluation[15] of 50,000 field mud reports, *R* varied statistically between 0.50 – 0.68 for synthetic-based muds, 0.48 – 0.59 for oil-based muds, and 0.20 – 0.40 for water-based muds, with the most likely values of 0.57, 0.50, and 0.30, respectively.

The same study generated typical *PV* and *YP* ranges as a function of mud weight that can be used to streamline the optimization process if desired. Temperature and pressure-dependent downhole densities are determined by numerical integration of the fluid column elements. Basic inputs include surface fluid density, fluid continuous phase (synthetic, oil, water, or brine), and the downhole temperature profile.

Temperature-dependent variable downhole properties are simulated for any given set of rheological properties and fluid densities. Both steady state and transient temperature profiles are calculated based on flow rate, geothermal gradient, well geometry and profile among others, and density and rheology profiles are continually updated.

Frictional pressure losses in the circulating system are calculated using Herschel-Bulkley models in laminar, transitional, and turbulent flow.[5] Drillstring eccentricity and rotational effects are included in *ECD* calculations. Eccentricity reduces annular pressure loss, and shifts the ECD curves downward in the Annular Hydraulic Window. However, eccentricity also increases *Qmin*, thereby narrowing the available flow-rate range. Field data suggests that drill-string rotation shifts ECD curves upwards. Rotation, however, also reduces *Qmin* by avoiding cuttings bed formation and helps remove beds when formed.

Several different models are available to determine the *Qmin* value based on hole-cleaning and barite-sag requirement for given fluid properties, well parameters and drilling rates.[16] Some models account for the effect of rotation and eccentricity, making them suitable for use in conventional, and in extended-reach and deviated wells.

Case Studies

Four wells were selected from the Gulf Mexico, North Sea and Alaska to illustrate how the computer program optimizes bit hydraulics when drilling fluid rheology is included as an integral part of the process. Table 3 summarizes key well data at an arbitrarily selected depth for each well. Mud weights presented in the table were measured during drilling at corresponding temperatures listed under Tm.

Notably, these wells were drilled and completed successfully using fluid and operating conditions based on conventional optimization processes and existing field practices. They are revisited in this paper to see if changes in fluid rheology could have improved bit hydraulics parameters under similar well conditions. Modifications to well and fluid design and economic considerations required to achieve the recommended rheologies are beyond the scope of this paper.

Annular Hydraulics and Bit Hydraulics Optimization Windows are used to illustrate optimization results. Matching tables that compare original and optimized values are provided for each case to present numerical results, including flow rates and relevant bit hydraulics parameters. Optimum rheological properties suggested by the program are based on 120°F for water-based muds and at 150°F for oil- and synthetic-based muds. Any special considerations are noted where appropriate.

Maximum bit hydraulic horsepower was selected as the optimization criterion of choice, though this theoretical goal was not achieved on any of the wells. In two cases, hole cleaning was the dominant concern, meaning that the recommended flow rate was increased to *Qmin*. In the other

two, operational constraints resulted in larger than desirable bit nozzles being used, which in turn caused less than optimal bit hydraulic horsepower.

Well A: Deepwater Gulf of Mexico. Project goals were to set a whipstock in an existing Gulf of Mexico well (4,845-ft water depth), mill a window in the 9⅝-in. casing at about 14,000 ft, and sidetrack using a rotary steerable assembly and an 8½ x 9⅞-in. under-reamer to evaluate a series of interesting sands. Lost circulation, hole cleaning, penetration rates, and stuck pipe were among the primary drilling concerns. The interval selected for analysis started at a depth of 15,120 ft. Rheological properties for the 12.7-lb/gal SBM mud were within ranges recommended for the well. Bit nozzles were 2 x 14/32-in. and 2 x 13/32-in.

The original bit hydraulics situation for this well and optimization results are presented graphically in Figs. 4a and 4b. Table 4 summarizes comparison between actual field and optimum rheologies, flow rate, and bit hydraulic parameters.

The Annular Hydraulics Window (Fig. 4a) compares equivalent circulating density at the casing shoe as a function of flow rate using actual field (dashed line) and optimized rheology (solid line). Both curves include the effects of cuttings in the flow stream. The upper and lower *ECD* bounds are indicated by horizontal lines placed at *FG* = 14.0 lb/gal and *ESD* = 13.07 lb/gal at the casing shoe, respectively.

Actual well and optimum flow rates and resulting *ECD*s are indicated by solid circles in the plot. As shown in Fig. 4a, the original flow rate was only slightly higher than that required for hole cleaning.

Flow rate limits are indicated by vertical lines for minimum and maximum values, where the dashed lines represent the original well conditions and the solid lines indicate calculated limits with optimized rheology. Both minimum flow-rate values are based on API recommendations. On the other hand, both maximum flow-rate values are defined by the available pump pressure illustrated in Fig. 4b.

Fig. 4b is the Bit Hydraulics Optimization Window for this case study. Pump pressure originally used in the field (4,000 psi) is maintained for the enhanced optimization process. The intersections of the original and revised parasitic lines with the pump pressure define the respective maximum available flow rates, although neither plays a key role in the hydraulics. The minimum flow rates are carried over from Fig. 4a.

Because of high parasitic losses, only a small fraction of the pump pressure was available at the bit. The program attempted to lower the *PV* as much as practical to help this cause, and suggested changing *PV/YP/*τ_y values from 25/22/19 to 10/28/24. This would reduce parasitic losses and increase *HHPb* by more than 128%. Because of practical limits on *PV* for this mud weight, optimum *HHPb* could not be achieved since *Qopt* was higher, but still less that *Qmin* for hole cleaning. Maximum jet velocity was the result, but this parameter would increase for 246 to 360 ft/s. Increased *YP* and τ_y to help hole cleaning played roles in this improvement.

A benefit of this type of analysis is increased opportunities for drilling fluid systems that exhibit advantageous rheological characteristics. Difficulties with running conventional weighted systems with very low *PV* values can be overcome by using a SBM with unconventional weight material, such as micronized barite specially treated to reduce surface area and rheology.[17] Field applications have proven that these unique fluids can reduce ECDs and barite sag tendencies, allow higher pump rates, and lower torque and drag.[18,19]

Well B: North Sea HTHP. This critical HTHP well was successfully drilled in the troublesome Central Graben trough between the UK and Norwegian sectors of the Central North Sea, but not before addressing potentially serious ECD management issues.[20] Drilling challenges for the vertical exploration well included very narrow operating windows (0.5-lb/gal and less) and the inability to run pressure-while-drilling tools due to high downhole temperatures. On-site hydraulics simulations were successfully executed to assist operations with maintaining proper ECD control and adequate hole cleaning.

The interval selected for post-well analysis was the 8½-in. hole just before setting a 7¾-in. liner. Intermediate 9⅞-in. casing had been set at about 14,000 ft to seal off weak upper zones. The narrow window created by the estimated 17.6-lb/gal pore pressure and 18.6-lb/gal fracture gradient raised simultaneous concerns with gas influx and lost circulation.

Hydraulics-related problems were avoided, despite the many tight constraints and potential drilling problems that over shadowed major bit hydraulics issues. Nevertheless, post-well analysis using the program described in this paper suggested opportunities for improving both ECD management and bit hydraulics performance.

Fig. 5a shows the annular hydraulic window using actual and suggested rheologies, and Table 5 presents key results in tabular form. The data indicate that major improvements could be realized by a significant reduction in *PV*. Slight increases in *YP* and τ_y could lower *Qmin* and increase available bit hydraulic horsepower by 38% as shown in Fig. 5b. This would allow a lower flow rate and lower ECDs to mitigate issues with the narrow drilling window without compromising hole cleaning. This figure also shows that optimum *HHPb* could not be achieved and maximum jet velocity would have to suffice. As such, *Pb* could only be increased only by about 10% to 31% of the pump pressure.

Based on the global database analysis presented earlier, the suggested PV value was lower than typical ranges for the low-toxicity oil-based mud using conventional API barite. This suggests another possible application of the micronized barite fluid system.

Well C: Alaska Horizontal ERD. As with many long-reach horizontal projects, this well faced hole cleaning and lost circulation challenges in a narrow operating window. Compromise among competing factors is often the best, and sometimes the only, approach. On occasion, even the best plans must be modified to handle drilling conditions.

The plan was to use a 9.9-lb/gal mineral-oil-based mud in the 6¾-in. horizontal section. Offset well data suggested that 280-310 gal/min was adequate for hole cleaning with *PV*s from 20-24 cP and *YP*s from 10-12 $lb_f/100ft^2$. A *TFA* of 0.69

in.^{2} was recommended for bit hydraulics to sustain reasonable penetration rates. High ECDs and lost circulation were potential concerns and that required larger hole and casing sizes than normally used in that region. Careful monitoring of rate of penetration, fluid rheology, and ECD trends were recommended in the plan to avoid hole-cleaning problems. The interval selected for analysis started at a depth of 11,200-ft just before running the 3½-in. slotted production liner.

The drilling plan had to be altered when 3 x 20/32-in. bit nozzles were used to avoid plugging since nut plug was added to the fluid to reduce vibrations while drilling in hard formations. This compromised bit hydraulic horsepower and resulted in a low pump pressure. Fig. 6a shows the annular hydraulic window, while Table 6 summarizes key results.

Drilling ECDs were not a concern due to a relatively high *FG* of 12.5-lb/gal. Fig. 6b is the bit hydraulics optimization window for this case study. Pressure loss through the bit was only 85 psi. Post-well analysis was performed to investigate if bit hydraulics could have been optimized by adjusting fluid rheology and flow rate to accommodate operational constraints. Pump pressure (2700 psi) and bit nozzles (3 x 20/32-in.) originally used in the field were maintained for the enhanced optimization process. As expected, the program suggested that a combination of higher flow rate and reduced parasitic losses could have improved bit hydraulics. This could be achieved by changing $PV/YP/\tau_y$ values from 24/9/5 to 10/10/6, and increasing flow rate from 280 to 327 gal/min. This would increase *HHPb* by more than 63%. Optimum *HHPb* could not be achieved since the rheology optimization was constrained by a combination of large bit nozzles and low pump pressure.

Well D: Alaska Injector. Project objective was to drill a Class I injector well in Alaska. The 8½-in. injection interval was planned to be completed with 7-in. liner. Potential problems included high torque and drag, and poor hole-cleaning in the intermediate section. Environmental restrictions required that the liner reach interval TD and have excellent cement bond. Based on offset well data, a low solids non-dispersed water-based mud (LSND) with a nominal mud weight of 9.2-lb/gal was approved to be used in the injection interval. Minor seepage losses while drilling necessitated the use of a mixture of medium-sized nut plug and fine fibrous lost circulation material. The drilling plan had to be suitably adjusted by using larger bit nozzles (6 x 13/32-in.) to avoid plugging. This compromised bit hydraulic horsepower and resulted in a low pump pressure.

The annular hydraulic window shown in Fig. 7a indicates that with actual rheologies, *ECD* at the last casing shoe was less than *FG*. Minor seepage losses experienced while drilling were probably due to the presence of micro fractures. Hole-cleaning problems were avoided since flow rate was always greater than *Qmin*. Pump pressure (2200 psi) and bit nozzles originally used in the field were maintained for the enhanced optimization process. Post-well analysis using the rheology optimization suggested changing $PV/YP/\tau_y$ from 12/31/17 to 5/20/11.2, and increasing flow rate from 550 to 648 gal/min. Fig. 7b shows that a combination of lower parasitic losses and higher flow rate can result in a more than 60% increase in *HHPb* even though optimal values still could not be achieved. Table 7 summarizes final rheology optimization results.

Conclusions

1. The hydraulic optimization process can be significantly improved by considering drilling fluid rheological properties as optimization targets.
2. Traditional hydraulic optimization techniques should include annular hydraulics concepts to ensure adequate hole cleaning and ECD limitations.
3. Rheology optimization processes generate recommended flow rates and the Herschel-Bulkley parameters n, k, and τ_y as measured at the surface using field VG meters.
4. The optimization process should consider complex downhole fluid behavior, even though the optimization output suggests rheological parameters as would be measured at the surface.
5. Optimization solutions must be based on iterative and convergence processes rather than full numerical techniques.
6. Analyses of the case studies clearly support the advantages of minimizing plastic viscosity whenever possible, and elevating yield stress for hole cleaning.
7. Drilling fluid design and research into development of unconventional systems and additives could be a by-product of the rheology optimization process.

Acknowledgements

The authors thank the management of M-I SWACO for supporting this work and for giving permission to publish. They also thank the engineers, field personnel, and computer scientists who helped develop this technology.

References

1. Bizanti, M.S. and Blick, E.F.: "Fluid Dynamics of Wellbore Bottomhole Cleaning," SPE 15010 presented at SPE Permian Basin Oil & Gas Recovery Conference, Midland, TX, 13-14 Mar 1986.
2. Sutko, A.A., Sifferman, T.R., Haden, E.L. and Wahl, H.A.: "How We Can Be More Efficient with Our Drilling Hydraulics," SPE 4971 presented at the SPE Annual Fall Meeting, Houston, 6-9 Oct 1974.
3. King, I., Wells, M.R., Pessier, R.C., and Besson, A.: "A Methodology Using Laboratory Experiments and Numerical Modeling to Optimize Roller Cone Bit Hydraulics," SPE 28315 presented at the SPE Annual Technical Conference & Exhibition, New Orleans, 25-28 Sept 1994.
4. Wells, M.R. and Pessier, R.C.: "The Effects of Bit Nozzle Geometry on the Performance of Drill Bits," AADE-03-NTCE-51 presented at the 2003 AADE National Technical Conference, Houston, 1-3 April 2003.
5. Kendall, H.A. and Goins, W.C.: "Design and Operation of Jet-Bit Programs for Maximum Hydraulic Horsepower, Impact Force or Jet Velocity," SPE 1288-G presented at the SPE Annual Fall Meeting, Dallas, 4-7 Oct 1959, and *AIME Petroleum Transactions*, v**219** (1960) 230, and *Petroleum Transactions Reprint Series*, No. 6 (Drilling).

6. Buckley, P. and Jardiolin, R.A.: "How to Simplify Rig Hydraulics," *Petroleum Engineer International* (Mar 1982) 154.
7. Doiron, H.H. and Deanne, J.D.: "A New Approach for Optimizing Bit Hydraulics," SPE 11677 presented at the SPE California Regional Meeting, Ventura, CA, 23-25 Mar 1983.
8. Bourgoyne, A.T., *et al.*: *Applied Drilling Engineering*, SPE, Richardson, Texas (1991).
9. *API Recommended Practice 13D: Rheology and Hydraulics of Oil-Well Drilling Fluids*, 5th ed.; American Petroleum Institute (June 2006).
10. Scott, K.F.: "A New Practical Approach to Rotary Drilling Hydraulics," SPE 3530 presented at the SPE Annual Fall Meeting, New Orleans, 3-6 Oct 1971.
11. Zamora, M. and Grundt, G.: "New Slide Rule Simplifies Bit Hydraulic Optimization," *Oil & Gas J*. (20 Jan 1975).
12. Randall, B.V.: "Optimum Hydraulics in the Oil Patch," *Petroleum Engineer* (Sept 1975) 36.
13. Swanson, B.W., Thorogood, J.L., and Gardner, A.: "The Design and Field Implementation of a Drilling Hydraulics Application for Drilling Optimization," SPE 27548 presented at the SPE European Petroleum Computer Conference, Aberdeen, 15-17 Mar 1994.
14. Hemphill, T.: "Integrated Management of the Safe Operating Window: Wellbore Stability is More Than Just Fluid Density," SPE 94732 presented at the SPE Latin American and Caribbean Petroleum Engineering Conference, Rio de Janeiro, 20-23 June 2005.
15. Power, D. and Zamora, M.: "Drilling Fluid Yield Stress: Management Techniques for Improved Understanding of Critical Drilling Fluid Parameters," AADE-03-NTCE-35 presented at the AADE National Technology Conference, Houston, 1-3 Apr 2003.
16. Luo, Y., *et al.*: "Flow Rate Predictions for Cleaning Deviated Wells," SPE 23884 presented at the IADC/SPE Drilling Conference, New Orleans, 18-21 Feb 1992.
17. Oakley, D.: "Specially Treated Drilling Fluid Weighting Agent Facilitates Development of Mature Reservoirs," AADE-06-DF-HO-27 presented at the AADE Drilling Fluids Technical Conference, Houston, 11-12 Apr 2006.
18. Fimreite, G., Asko, A., Massam, J., Taugbol, K.,, Omland, T.H., Svanes, K., Andreassen, E., and Saases, A.: "Invert Emulsion Fluids for Drilling Through Narrow Hydraulic Windows," IADC/SPE 87128 presented at the SPE/IADC Annual Drilling Conference, Dallas, 2-4 Mar 2004.
19. Bolivar, N., Young, J., Dear, S., Massam, J., and Reid T.: "Field Result of Equivalent Circulating Density Reduction with a Low-Rheology Fluid," SPE/IADC 105487 presented at the SPE/IADC Drilling Conference, Amsterdam, 20-22 Feb 2007.
20. Thorsrud, A. K., Ekeli, O., Hilbig, N. C. C., Bergsvik, O., and Zamora, M.: "Application of Novel Downhole Hydraulics Software to Drill Safely and Economically a North Sea High-Temperature/High-Pressure Exploration Well," IADC/SPE 59189 presented at the IADC/SPE Asia Pacific Drilling Technology Conference, Malaysia, 11-13 Sept 2000.

Nomenclature and Abbreviations

ECD	=	Equivalent circulating density, lb/gal
ESD	=	Equivalent static density, lb/gal
FG	=	Fracture gradient, lb/gal
HHPb	=	Bit hydraulic horsepower, hp
HHPp	=	Pump hydraulic horsepower, hp
HSI	=	Bit hydraulic horsepower/in.^{2}, hp/in.^{2}
HTHP	=	High-temperature/high-pressure
IFb	=	Bit Impact Force, lb_f
k	=	Herschel-Bulkley consistency factor, $lb_f \cdot s^n/100\ ft^2$
LTOBM	=	Low-toxicity oil-based drilling mud
MW	=	Mud weight, lb/gal
n	=	Herschel-Bulkley flow-behavior index, dimensionless
Pb	=	Pressure loss through bit nozzles, psi
Pp	=	Pump pressure, psi
PV	=	Plastic viscosity, cP
Q	=	Flow rate, gal/min
Qmax	=	Maximum flow rate, gal/min
Qmin	=	Minimum flow rate, gal/min
Qopt	=	Optimum flow rate, gal/min
Qrec	=	Recommended flow rate, gal/min
R	=	Ratio of yield stress/yield point
ROP	=	Rate of penetration, ft/hr
s	=	Turbulent flow behavior index, dimensionless
SBM	=	Synthetic-based drilling mud
Tm	=	Temperature for mud weight measurement, °F
TD	=	Total depth (measured), ft
TFA	=	Total nozzle flow area, in.^{2}
TVD	=	True vertical depth, ft
WBM	=	Water-based drilling mud
WD	=	Water depth, ft
YP	=	Yield point, $lb_f/100\ ft^2$
τ_y	=	Yield stress, $lb_f/100\ ft^2$

Table 1 – Effect of turbulent flow index on Pb as percent of pump pressure for optimization

Exponent s =	1.3	1.4	1.5	1.6	1.7	1.8	1.9
Optimum HHPb	56.5	58.3	60.0	61.5	63.0	64.3	65.5
Optimum IFb	39.4	41.2	42.9	44.4	45.9	47.4	48.7

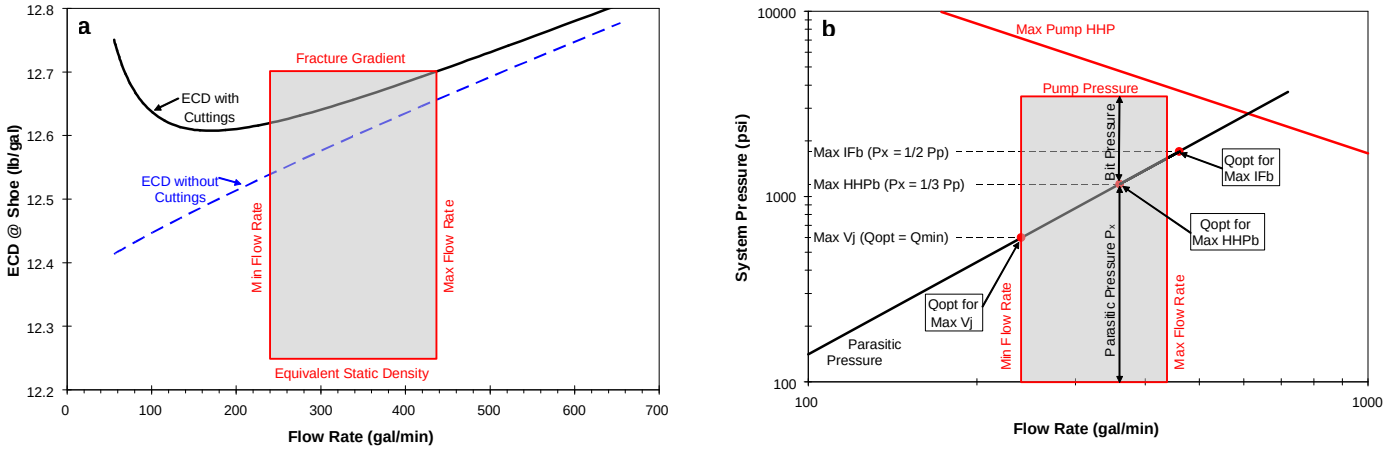

Figs. 1a-1b. Example Annular Hydraulics and Bit Hydraulics Optimization Windows.

Table 2 – Summary results for the example windows in Figs. 1a-1b												
PV cp	**YP** $lb_f/100\ ft^2$	**τ_y** $lb_f/100\ ft^2$	**Q** gal/min	**Qmin / Qmax** gal/min	**TFA** in^2	**Pb** psi (%Pp)	**Pp** psi	**ECD_{shoe}** lb/gal	**HHPb** hhp	**HSI** hhp/in^2	**IFb** lb_f	**Vj** ft/s
20	14	8.1	360	240 / 436	0.236	2180 (62)	3500	12.67	458	8.07	1007	499

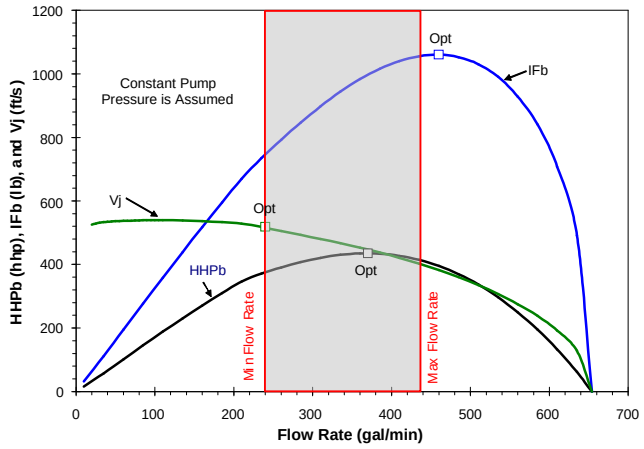

Fig. 2 – HHPb, IFb, and Vj at constant pump pressure as functions of flow rate.

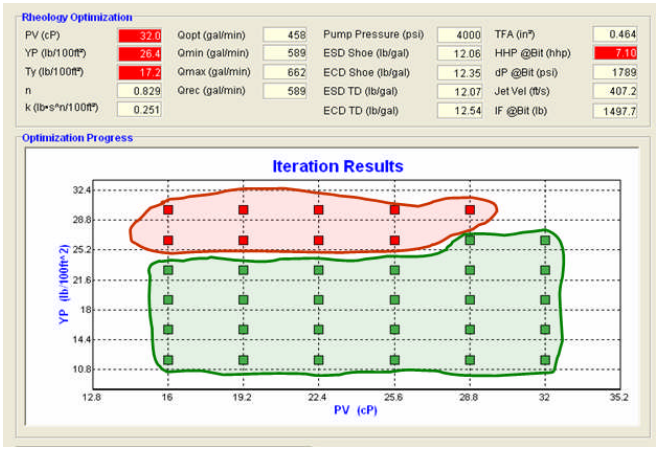

Fig. 3 – Example of iterative process used to evaluate PV and YP combinations on optimization. Upper enclosed set failed the criteria during this iteration; lower set passed.

Table 3 – Well identification and key properties for case studies												
Well ID	**Location**	**WD** ft	**TD** ft	**TVD** ft	**Hole Size** in.	**Csg Shoe** ft	**Csg OD** in.	**Mud Type**	**MW** lb/gal	**Tm** °F	**ROP** ft/hr	**FG** lb/gal
A	Gulf of Mexico	4,850	15,120	14,882	9⅞	14,000	9⅝	SBM	12.7	105	160	14.0
B	North Sea	238	15,600	14,902	8½	13,956	9⅞	LTOBM	17.8	101	120	18.6
C	Alaska	0	11,200	4,067	6¾	5,561	7⅝	LTOBM	9.9	88	95	12.5
D	Alaska	0	11,370	5,223	8½	8,296	9⅝	LSND	9.2	85	150	11.5

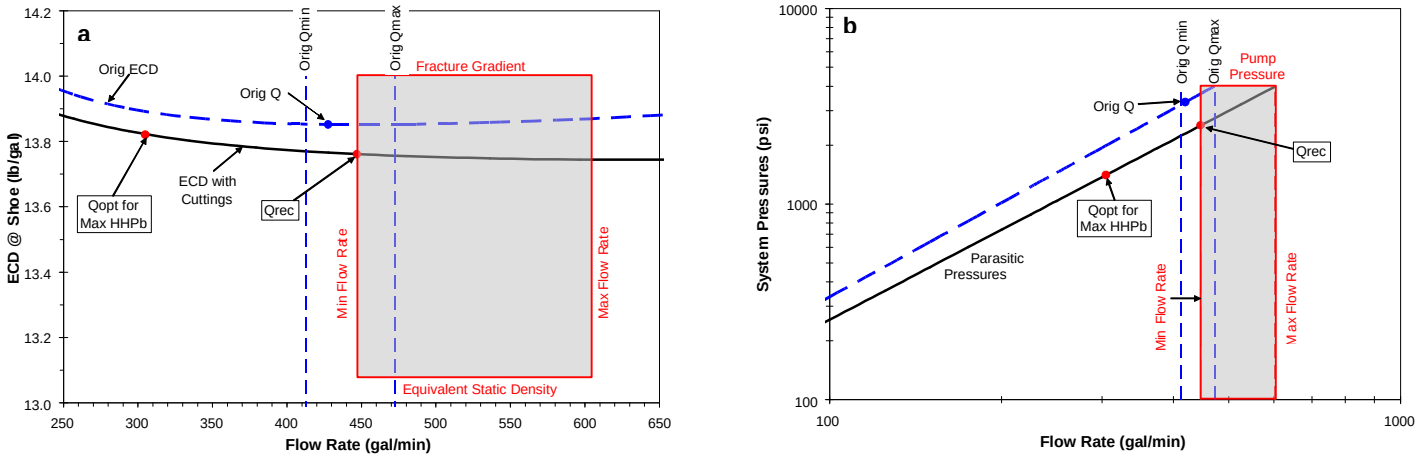

Figs. 4a-4b – Annular Hydraulics and Bit Hydraulics Optimization Windows for Well A (Gulf of Mexico Deepwater). Actual field data is shown by the dashed line and optimized rheology by the solid line.

Table 4 – Summary results for Well A (Gulf of Mexico Deepwater).

	PV cp	YP $lb_f/100\ ft^2$	τ_y $lb_f/100\ ft^2$	Q gal/min	Qmin / Qmax gal/min	TFA in^2	Pb psi (%Pp)	Pp psi	ECD_{shoe} lb/gal	HHPb hhp	HSI hhp/in^2	IFb lb_f	Vj ft/s
Orig	25	22	19	420	413 / 473	0.560	671 (17)	4000	13.85	164	2.15	672	246
Opt	10	28	24	447	447 / 604	0.407	1439 (36)	4000	13.76	375	4.90	1047	360

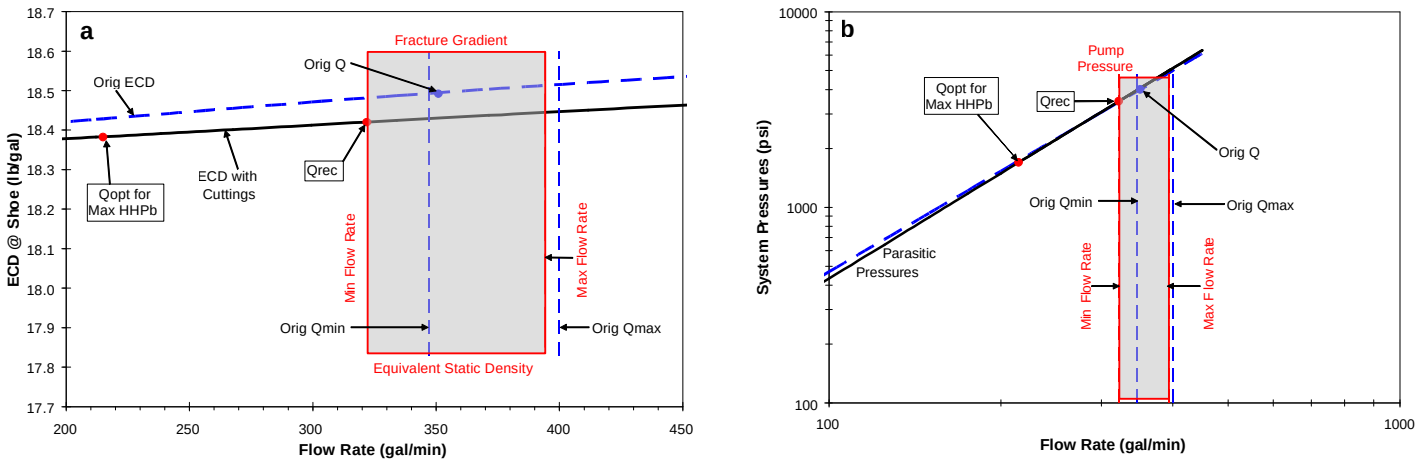

Figs. 5a-5b – Annular Hydraulics and Bit Hydraulics Optimization Windows for Well B (North Sea HTHP).

Table 5 – Summary results for Well B (North Sea HTHP)

	PV cp	YP $lb_f/100\ ft^2$	τ_y $lb_f/100\ ft^2$	Q gal/min	Qmin / Qmax gal/min	TFA in^2	Pb psi (%Pp)	Pp psi	ECD_{shoe} lb/gal	HHPb hhp	HSI hhp/in^2	IFb lb_f	Vj ft/s
Orig	47	14	7.0	351	347 / 400	0.442	1039 (21)	5000	18.47	213	3.75	826	260
Opt	30	15	7.5	322	322 / 395	0.331	1559 (31)	5000	18.44	293	5.16	928	318

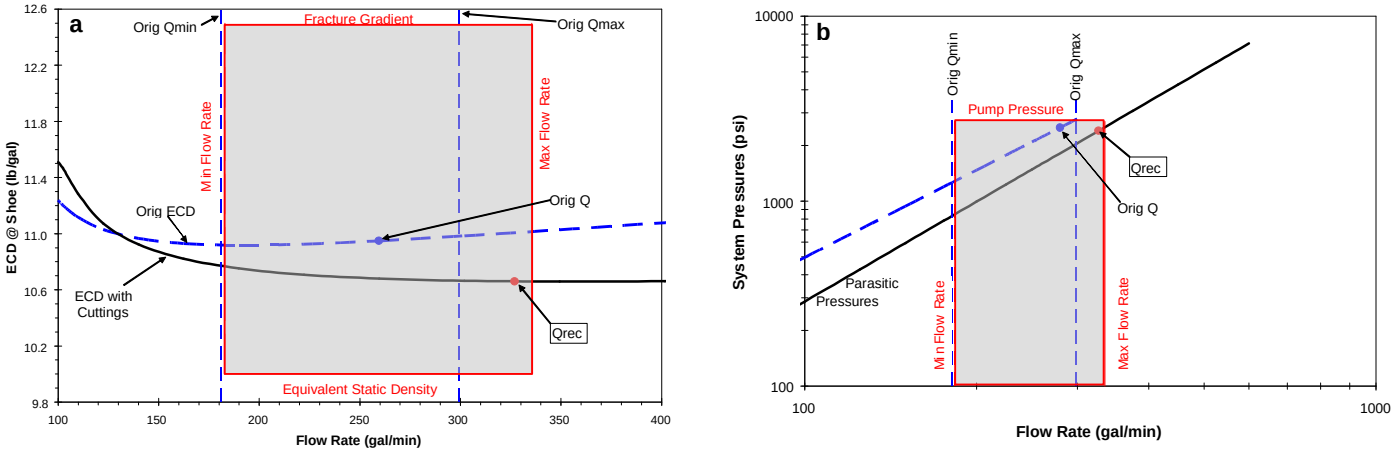

Figs. 6a-6b – Annular Hydraulics and Bit Hydraulics Optimization Windows for Well C (Alaska ERD).

Table 6 – Summary results for Well C (Alaska ERD)													
	PV cp	**YP** $lb_f/100\ ft^2$	**τ_y** $lb_f/100\ ft^2$	**Q** gal/min	**Qmin / Qmax** gal/min	**TFA** in^2	**Pb** psi (%Pp)	**Pp** psi	**ECD_{shoe}** lb/gal	**HHPb** hhp	**HSI** hhp/in^2	**IFb** lb_f	**Vj** ft/s
Orig	24	9	5.0	280	181 / 300	0.920	85 (3)	2700	10.89	13.9	0.38	141	100
Opt	10	10	5.7	327	183 / 335	0.920	116 (4)	2700	10.61	22.2	0.62	192	116

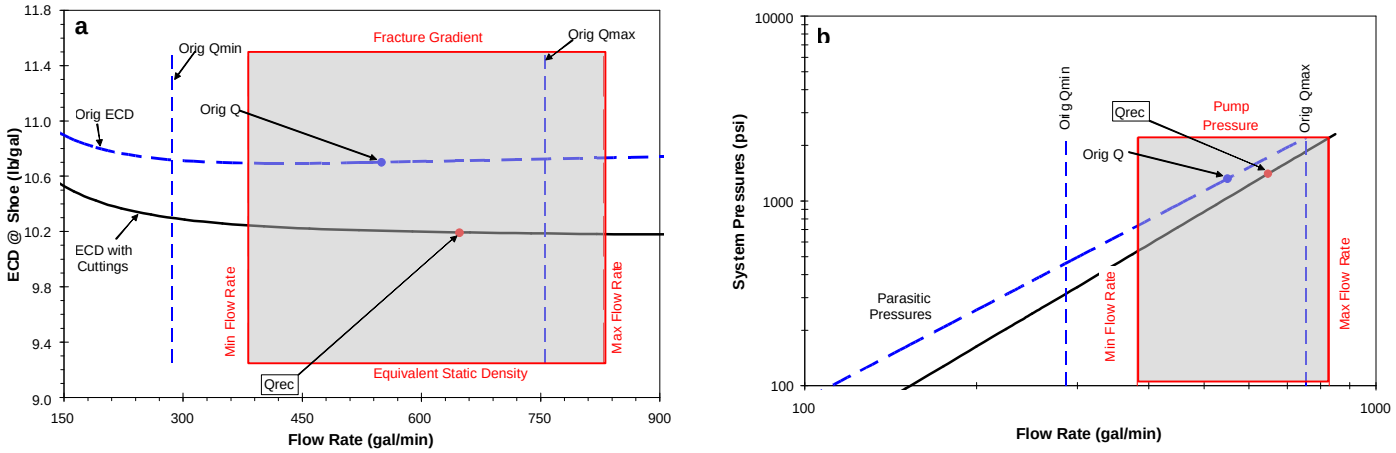

Figs. 7a-7b – Annular Hydraulics and Bit Hydraulics Optimization Windows for Well D (Alaska Injector).

Table 7. Summary results for Well D (Alaska Injector).													
	PV cp	**YP** $lb_f/100\ ft^2$	**τ_y** $lb_f/100\ ft^2$	**Q** gal/min	**Qmin / Qmax** gal/min	**TFA** in^2	**Pb** psi (%Pp)	**Pp** psi	**ECD_{shoe}** lb/gal	**HHPb** hhp	**HSI** hhp/in^2	**IFb** lb_f	**Vj** ft/s
Orig	12	31	17.0	550	286 / 755	0.778	425 (19)	2200	10.70	136	2.40	595	231
Opt	5	20	11.2	648	382 / 829	0.778	589 (27)	2200	10.18	223	3.92	825	273